

EUROPEAN ORGANIZATION FOR NUCLEAR RESEARCH
European Laboratory for Particle Physics



Internal NOTE

ALICE reference number
ALICE-INT-2009-021 version 1.0

Date of last change
November, 2009

The pixel detector based tracklet reconstruction algorithm in ALICE

D. Elia^a, J.F. Grosse-Oetringhaus^b, M. Nicassio^a, T. Virgili^c

a. Sezione INFN, Bari, Italy

b. CERN, European Organization for Nuclear Research, Geneva, Switzerland

c. Dipartimento di Fisica dell'Università and Sezione INFN, Salerno, Italy

Abstract

This note describes a method to reconstruct signals in the two silicon pixel detector layers compatible with tracks coming from the main interaction vertex, namely tracklets. The basic algorithm strategy and its performance are illustrated.

1 Introduction

The aim of this note is to describe a procedure that uses the clusters (that mainly correspond to reconstructed particle hits) in the two innermost layers of the Inner Tracking System (ITS) [1] to extract signals corresponding to charged tracks coming from the main interaction vertex. Those layers are equipped with silicon pixels and constitute the Silicon Pixel Detector (SPD): their average distances from the beam line are 3.9 and 7.6 cm with a pseudorapidity coverage of $|\eta| < 2$ and $|\eta| < 1.4$ respectively, as defined for particles originating in the centre of the detector. Further details on the detector design and the expected performance can be found in Ref. [2].

The reconstructed signals (tracklets) will be used to estimate the number of primary charged particles produced both in proton-proton and heavy-ion collisions at ALICE [3]. Compared to the corresponding measurement based on the fully reconstructed tracks (using combined measurements from the ITS and the Time Projection Chamber) the charged-particle multiplicity reconstructed only with pixels has some basic advantages: a larger acceptance coverage both in pseudorapidity and p_T (down to 30 MeV/ c) and a much smaller reliance on alignment and calibration procedures. This makes the measurement with SPD tracklets suitable to extract results from the very first available data from the LHC. The note is organized as follows. Section 2 deals with the description of the tracklet algorithm used for the ALICE Physics Performance Report [3]: studies on the optimization of the cuts for the tracklet definition and the performance of the method both for p-p and Pb-Pb simulated collisions are presented. In Section 3 a recent update of the algorithm strategy and of the cut variables is discussed, including a comparison with the original method. The fine tuning of the algorithm is discussed in Section 4. Finally, Section 5 illustrates a procedure to eliminate tracklet duplication (same physical track) due to overlapping regions between sensitive areas of the detector and Section 6 summarizes the note.

2 The tracklet reconstruction algorithm

In this section the algorithm to estimate the charged particle multiplicity using data from the SPD only, namely the tracklet algorithm, is described. The reconstructed points of the SPD (clusters¹) and the reconstructed main vertex position are needed to build tracklets. The primary vertex is reconstructed using SPD clusters as well, exploiting their correlation as described in Refs. [4, 5].

¹A cluster is made up of one or more hit adjacent pixels.

A straight line from the vertex to each cluster in the inner layer is considered. For each cluster in the inner layer two differences are computed using the reconstructed vertex as the origin: the difference in the azimuthal angles ($\Delta\varphi$) between this cluster and each cluster in the outer layer and the difference between the longitudinal coordinate of the prediction from the straight line in the outer layer and the longitudinal coordinate of each cluster in the outer layer ($\Delta z_{projected}$). The differences are schematically shown below in Fig. 1.

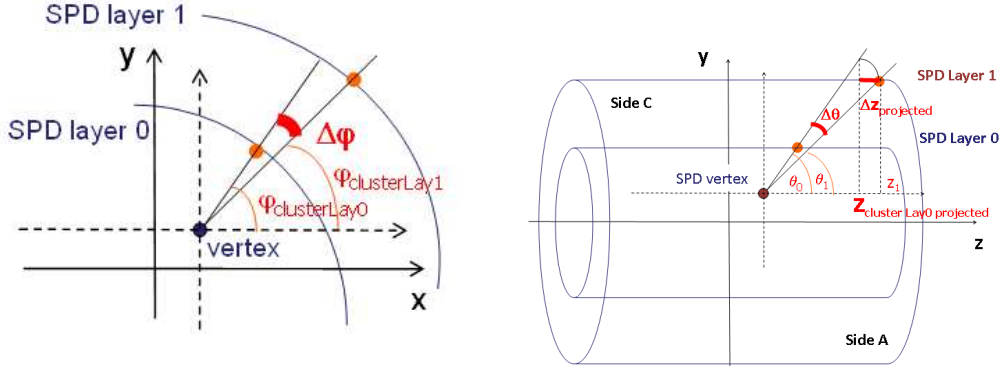


Figure 1: Sketch of the two differences calculated for each combination of clusters in the two SPD layers used to define tracklets: the transverse plane view of the detector (left panel) illustrates how the $\Delta\varphi$ is calculated and the z - y plane view (right panel) illustrates how the $\Delta z_{projected}$ is calculated (approximation of the prediction of the straight line in the outer layer).

Regarding the $\Delta z_{projected}$, it should be noticed that the prediction on the outer layer cannot be precisely determined since the position of the module in that point cannot be retrieved, therefore an approximation is used, as it can be seen in Fig. 1. It turns out that this variable is not constant as θ varies, keeping $\Delta\theta$ constant: it is bigger if the pseudorapidity $|\eta|$ of the cluster in the outer layer increases. For each pair an elliptical cut is applied and if the pair satisfies the window requirement, it is labeled as “tracklet” [3, 6]. If more than one cluster in the outer layer matches the window requirement with the same cluster in the inner layer, the one with the minimum distance is associated to the cluster in the inner layer. The procedure is repeated for each cluster in the inner layer so that each cluster can be associated only once. Clusters in the outer layer can either be used in one tracklet only or in more than one. In the first case it turns out that the reconstructed tracklets are biased by the cluster ordering². The default widths of the cut windows for p-p events are $\Delta\varphi_{cut} = 0.08$ rad and $\Delta z_{cut} = 1$ cm respectively. The cut imposed in the azimuthal angle corresponds to a transverse-momentum cut-off of about 35 MeV/c (for

²The ITS clusters are ordered according to the increasing number of the module they belong and in the module according to the increasing z and φ .

pions). The possibility to interpolate starting from the clusters on the outer layer has been also considered [6]: due to the larger background fraction on that layer, the number of fake tracklets is larger in this case, especially for Pb-Pb events.

The pseudorapidity η is evaluated by considering a straight line from the main vertex to the position of the cluster in the inner layer. The multiplicity of charged particles is estimated counting the number of tracklets. This number has to be corrected for several effects, as described in Refs. [7, 8].

The tracklet-based method for multiplicity studies is a proven technique used in the PHOBOS experiment at RHIC [9]. The tracklet method allows a good rejection of the background (detector noise, secondary particles, residual beam-gas contamination): in particular for p-p collisions, due to the relatively low multiplicity, the background induced statistical fluctuations have to be considered not negligible compared to the signal.

2.1 Optimization of the cuts

Studies on the performance of the tracklet algorithm as a function of the selected fiducial windows and the adopted combination strategy will be presented in this and in the next section. All these studies have been carried out using three different Monte Carlo collision samples listed below:

- 10000 Pythia minimum bias p-p events at $\sqrt{s} = 14$ TeV;
- 5000 Hijing minimum bias Pb-Pb events at $\sqrt{s_{NN}} = 5.5$ TeV;
- 1000 Hijing 5% most central Pb-Pb events at $\sqrt{s_{NN}} = 5.5$ TeV.

The magnetic field has been assumed at the nominal ALICE value of 0.5 Tesla.

The widths of the cuts applied have to be optimized with respect to the efficiency in reconstructing primary particles and the background contamination. A performance study has been carried out varying the cuts applied both for p-p and Pb-Pb events (minimum bias and central). The Monte Carlo particle labels stored in the reconstruction process for the two clusters that made up each tracklet are used for this purpose. In order to choose a reasonable set of cuts, the signal, i.e. pairs of clusters produced each by the same primary particle, has been plotted in the $\Delta\varphi$ - $\Delta z_{projected}$ plane both for p-p and for Pb-Pb events. In Fig. 2 the result for central Pb-Pb events is shown.

The efficiency has been evaluated as the ratio between all the reconstructed primaries, i.e. primaries that have a tracklet associated, and all the primaries that produced at least one cluster in each layer. In order not to include in this efficiency the effect of the vertex reconstruction quality, events with a reconstructed vertex in $|z_{vtx}| < 10$ cm are

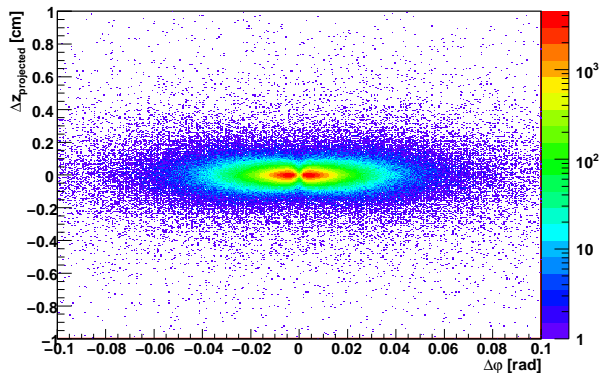


Figure 2: $\Delta\varphi$ and $\Delta z_{projected}$ for pairs of clusters by the same primary particle in central Pb-Pb events.

considered. Indeed events with a bad reconstructed vertex would lower the efficiency since the two cluster produced cannot be aligned with the vertex within the fiducial windows. In addition, the reconstructed tracklets have been classified as primary, secondary tracklets or combinatorics. The efficiencies and the percentages in the tracklet composition are shown in Tab. 1 for p-p events. The results allowing multiple association of clusters in the outer layer are quoted in brackets. Preventing multiple associations, the efficiency

$\Delta\varphi_{cut}$ (rad)	Δz_{cut} (cm)	Efficiency (%)	PP (%)	SS (%)	Combinatorics (%)
0.0800	1.00	97.4 (98.8)	89.9 (88.5)	5.9 (5.8)	4.2 (5.7)
0.0800	0.50	98.2 (98.6)	92.4 (91.8)	5.4 (5.4)	2.2 (2.8)
0.0800	0.30	98.2 (98.5)	93.5 (93.1)	4.8 (4.9)	1.6 (2.0)
0.0800	0.20	98.0 (98.2)	94.3 (94.0)	4.4 (4.4)	1.3 (1.6)
0.0600	0.20	97.7 (97.9)	94.7 (94.5)	4.1 (4.1)	1.2 (1.4)
0.0400	0.10	95.6 (95.6)	96.2 (96.1)	3.1 (3.1)	0.7 (0.8)
0.0200	0.05	84.8 (84.8)	97.5 (97.4)	2.1 (2.1)	0.4 (0.5)
0.0150	0.03	69.8 (69.8)	97.9 (97.8)	1.7 (1.8)	0.4 (0.4)
0.0100	0.02	51.1 (51.1)	98.1 (98.1)	1.6 (1.6)	0.3 (0.3)
0.0075	0.01	27.8 (27.8)	98.2 (98.3)	1.4 (1.4)	0.4 (0.3)

Table 1: Efficiency of the tracklet algorithm and tracklet composition varying the cuts to reconstruct tracklets for the Monte Carlo p-p sample. In brackets the results allowing multiple association of clusters in the outer layer are quoted.

increases and then decreases as the cuts become tighter. Allowing multiple association the efficiency has the expected trend. Furthermore, in the latter case the efficiencies are higher and the combinatorics is lower, due to the fact that the order does not prevent the algorithm from sorting the best association. However the results obtained with the two options do not differ as the cuts become tighter. The order dependence can be clearly

seen in Fig. 3, where the comparison between the $\Delta\varphi$ distribution of tracklets obtained preventing and allowing multiple association of clusters in the outer layer is shown.

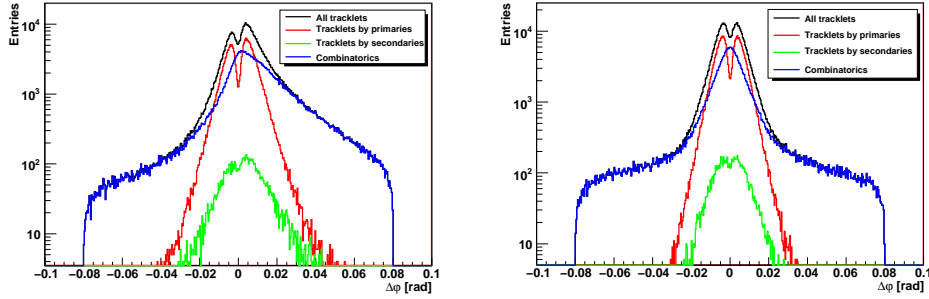


Figure 3: $\Delta\varphi$ distributions of tracklets reconstructed preventing (left panel) and allowing (right panel) multiple association of clusters in the outer layer for the Monte Carlo sample of central Pb-Pb events.

In Tab. 2 and Tab. 3, the efficiencies and tracklet compositions are quoted for minimum bias and central Pb-Pb events respectively. For Pb-Pb events the maximum achievable

$\Delta\varphi_{cut}$ (rad)	Δz_{cut} (cm)	Efficiency (%)	PP (%)	SS (%)	Combinatorics (%)
0.0800	1.000	51.5 (74.3)	39.0 (48.6)	1.7 (1.7)	59.3 (49.7)
0.0800	0.200	63.3 (74.6)	54.0 (61.6)	2.1 (2.1)	43.9 (36.3)
0.0150	0.030	60.2 (61.1)	86.4 (85.1)	1.7 (1.7)	11.9 (13.2)
0.0125	0.025	52.5 (53.2)	87.7 (86.5)	1.6 (1.6)	10.7 (11.9)
0.0100	0.020	42.1 (42.5)	88.6 (87.8)	1.5 (1.5)	9.9 (10.7)
0.0075	0.015	28.6 (28.7)	89.1 (88.6)	1.4 (1.4)	9.5 (10.0)
0.0060	0.005	9.9 (9.9)	89.8 (89.6)	1.3 (1.3)	8.9 (9.1)

Table 2: Efficiency of the tracklet algorithm and tracklet composition varying the cuts for tracklet reconstruction of the minimum bias PbPb sample. The results allowing multiple association of clusters in the outer layer are quoted in brackets.

efficiency is quite low and the background fraction is high, in particular for central events where the maximum efficiency is about 60% and half of the reconstructed tracklets are combinatorics. These emerged features suggested that there was room for improving the algorithm performance.

3 Optimization of the tracklet algorithm

In principle, the best algorithm should associate the pair with the minimum distance over all the possible combinations of clusters in the inner layer with clusters in the outer layer. Such an algorithm would be time-consuming. Alternatively, an iterative procedure,

$\Delta\varphi_{cut}$ (rad)	Δz_{cut} (cm)	Efficiency (%)	PP (%)	SS (%)	Combinatorics (%)
0.0800	1.000	42.0 (63.4)	31.9 (42.3)	1.1 (1.2)	67.0 (56.5)
0.0800	0.200	50.3 (63.5)	42.2 (53.0)	1.4 (1.4)	56.4 (45.5)
0.0150	0.030	55.8 (57.1)	79.2 (77.4)	1.5 (1.5)	19.3 (21.1)
0.0125	0.025	49.1 (50.1)	81.0 (79.5)	1.5 (1.4)	17.5 (19.1)
0.0100	0.020	39.6 (40.3)	82.5 (81.3)	1.4 (1.4)	16.1 (17.3)
0.0075	0.015	27.0 (27.3)	83.1 (82.4)	1.3 (1.3)	15.6 (16.3)
0.0060	0.005	9.2 (9.3)	84.2 (83.8)	1.3 (1.3)	14.5 (14.9)

Table 3: *Efficiency of the tracklet algorithm and tracklet composition varying the cuts for the sample of central Pb-Pb events. The results allowing multiple association of clusters in the outer layer are quoted in brackets.*

starting from the basic algorithm, can be implemented. The first step is basically the old algorithm allowing multiple use of clusters in the outer layer. At the end of the loop on clusters in the inner layer, outer layer clusters, associated to more than one cluster in the inner layer, have to be associated to the only cluster in the inner layer with which each has the minimum distance. This basic block should be repeated using all the clusters not associated in the previous step. The iterations stop when no more tracklets are found.

Concerning the cut variables, the cut in $\Delta z_{projected}$ can be replaced with a cut in $\Delta\theta$, that is constant varying θ (Fig. 4). As for the cut in $\Delta\varphi$, when the magnetic field is

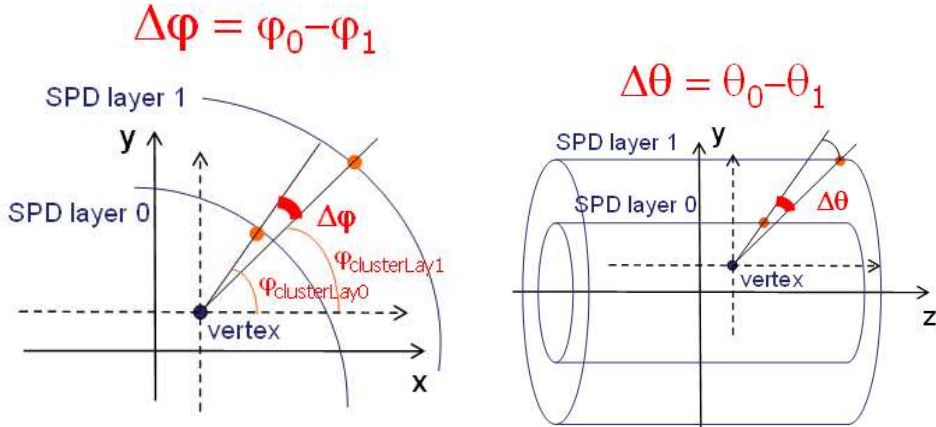


Figure 4: *Sketch of the two differences calculated for each combination of clusters in the two SPD layers used in the optimized tracklet algorithm: the transverse plane view of the detector (left panel) illustrates how the $\Delta\varphi$ is calculated and the z - y plane view (right panel) illustrates how the $\Delta\theta$ is calculated.*

on in the simulation, the $\Delta\varphi$ distribution of the reconstructed tracklets has two peaks due to the charge of the reconstructed particles (primaries and secondaries). In Fig. 5

an example of $\Delta\varphi$ distributions of tracklets reconstructed with the magnetic field on and without magnetic field are shown. Thus, according to the value of the magnetic field, a shift can be added in the calculation of the $\Delta\varphi$. A linear $\Delta\varphi$ dependence on the magnetic field has been assumed.

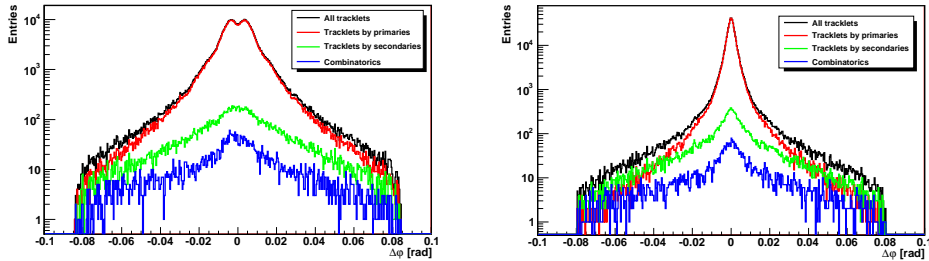


Figure 5: $\Delta\varphi$ distributions for tracklets reconstructed in a sample of p - p Monte Carlo events generated with magnetic field $B = 0.5$ T (left panel) and with magnetic field $B = 0$ T (right panel).

This procedure shows better performance than the basic algorithm, in particular in reconstructing Pb-Pb events: the efficiency is higher and the background contamination markedly decreases. In Tab. 4 the efficiency and tracklet composition for one set of cuts are shown both for the basic and the iterative algorithm for central Pb-Pb events.

	$\Delta\varphi_{cut}$ (rad)	$\Delta\theta_{cut}$ (rad)	Efficiency (%)	PP (%)	SS (%)	Combinatorics (%)
Old	0.08	0.025	63.5	53.0	1.4	45.5
New	0.08	0.025	74.7	64.5	1.9	33.6

Table 4: Comparison of the efficiency and tracklet composition between the optimized tracklet algorithm and the basic algorithm for the sample of central Pb-Pb events. For the old algorithm the $\Delta\theta_{cut}$ roughly corresponds to $\Delta z_{cut} = 0.2$ cm.

4 Tuning of the tracklet reconstruction

4.1 Tuning of the tracklet reconstruction in p-p events

In Fig. 6 the signal in the $\Delta\varphi$ - $\Delta\theta$ plane for p - p events is shown, while in Tab. 5 the optimized algorithm efficiencies are quoted for five sets of cuts.

As explained in Section 2.1, the efficiencies and the background contaminations have been calculated using events with a vertex reconstructed in $|z_{vtx}| < 10$ cm. The $\Delta\theta_{cut} = 0.15$ rad corresponds roughly to the $\Delta z_{cut} = 1$ cm at $\theta = \pi/2$ rad. The efficiency is not much higher than with the old algorithm because of the low SPD occupancy in p - p

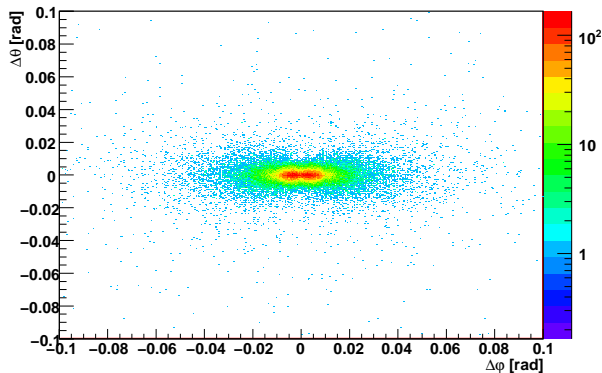


Figure 6: $\Delta\varphi$ and $\Delta\theta$ for pairs of clusters produced by the same primary particle in p - p events.

$\Delta\varphi_{cut}$ (rad)	$\Delta\theta_{cut}$ (rad)	Efficiency (%)	PP (%)	SS (%)	Combinatorics (%)
0.08	0.150	98.7	91.3	6.0	2.7
0.08	0.050	98.7	93.6	5.1	1.3
0.08	0.025	98.2	94.8	4.3	0.9
0.04	0.005	85.0	97.2	2.4	0.4
0.02	0.005	79.3	97.7	1.9	0.4

Table 5: Efficiency of the optimized tracklet algorithm and tracklet composition varying the cuts to reconstruct the p - p event sample.

events, whereas the background fraction is a few percents lower. Tightening the applied cuts to $\Delta\theta_{cut} = 0.025$ rad and $\Delta\varphi_{cut} = 0.08$ rad, the efficiency decreases of .5 % only and the background fraction (secondary tracklets and combinatorics) is 3.5 % lower. A lower background fraction is preferable to a higher efficiency: indeed the background amount can depend on multiplicity hence on the Monte Carlo generator, efficiency, on the other hand, only depends on the cuts applied and can be easily taken into account in the correction to the multiplicity and pseudorapidity density distributions.

4.2 Tuning of the tracklet reconstruction in Pb-Pb events

As previously seen, the reconstruction of Pb-Pb events is very critical since the cluster occupancy in the SPD and the background are quite high. In particular in the 5% most central collisions, the mean number of clusters is about 21000 and 24000 in the SPD inner and outer layer respectively. The mean number of clusters from secondary particles 2600. In Fig. 7 the signal in the $\Delta\varphi$ - $\Delta\theta$ plane is shown for central events. A similar plot has been obtained for minimum bias events.

In Tab. 6 and Tab. 7 the efficiencies and the tracklet composition are shown for all

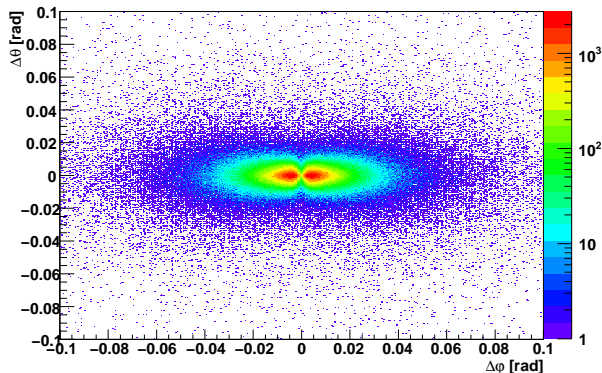


Figure 7: $\Delta\varphi$ and $\Delta\theta$ calculated for pairs of clusters produced by the same primary particle in central Pb-Pb events.

the cuts used to reconstruct tracklets in the minimum bias and central Pb-Pb events respectively.

$\Delta\varphi_{cut}$ (rad)	$\Delta\theta_{cut}$ (rad)	Efficiency (%)	PP (%)	SS (%)	Combinatorics (%)
0.08	0.150	71.2	56.1	2.1	41.8
0.08	0.050	81.2	68.2	2.6	29.2
0.08	0.025	83.2	72.8	2.6	24.6
0.04	0.005	73.6	82.3	2.1	15.6
0.02	0.005	70.0	86.5	1.9	11.6

Table 6: Efficiency of the optimized tracklet algorithm and tracklet composition varying the cuts to reconstruct the minimum bias PbPb event sample.

The efficiency increases and then decreases as the fiducial cuts become tighter because the larger windows used do not follow the elliptical correlation in the plane where the distance is computed. Having a high SPD cluster occupancy, wrong associations of clusters can have a smaller distance than the correct combination. In addition, the predominance of wrong combinations explains the background decrease as well. This does not happen for p-p events because the SPD cluster occupancy is low and, even using a large cut window, the probability to make wrong associations is low.

5 Study on the reconstruction in the SPD overlap regions

Due to the SPD geometry design, particles crossing the overlap regions between modules in φ can produce two clusters in each layer so that the track could be reconstructed twice. That happens more likely when the overlap region crossed are in the same sector,

$\Delta\varphi_{cut}$ (rad)	$\Delta\theta_{cut}$ (rad)	Efficiency (%)	PP (%)	SS (%)	Combinatorics (%)
0.08	0.150	59.3	47.4	1.4	51.2
0.08	0.050	71.9	60.3	1.8	37.9
0.08	0.025	74.7	64.5	1.9	33.6
0.04	0.005	67.2	73.7	1.8	24.5
0.02	0.005	64.8	79.4	1.7	18.9

Table 7: *Efficiency of the optimized tracklet algorithm and tracklet composition varying the cuts to reconstruct the central Pb-Pb event sample.*

while when the overlapping modules belong to adjacent sectors, the probability is smaller because the overlapping areas are smaller. The effect of the overlaps between the SPD modules in φ can be clearly seen in Fig. 8 for clusters, where the higher spikes are due to the overlap between modules in the same sector and the lower ones to the overlap between modules in adjacent sectors. In Fig. 9 the φ distribution for tracklets is shown as well.

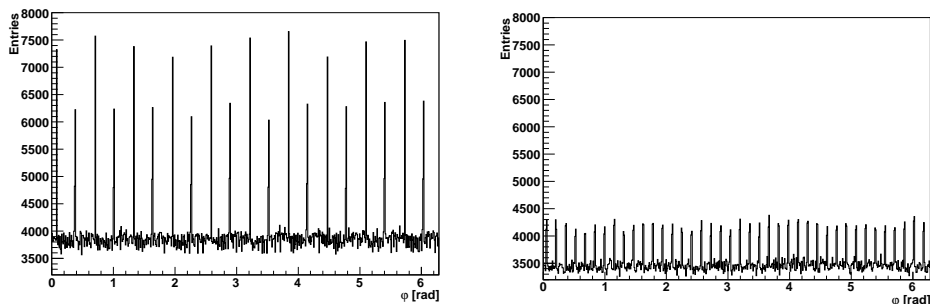


Figure 8: φ distributions for clusters in the inner layer (left panel) and in the outer layer (right panel): the spikes are due to overlaps between two SPD modules adjacent in φ .

This feature can be useful to check alignments with first data since the overlaps are 2% of the whole SPD. However, the multiple reconstruction of tracks can be limited: a procedure can be implemented to eliminate multiple reconstructed tracklets.

For each cluster, the basic idea is to look for clusters close enough to it in a module adjacent to the one it belongs, then flag them to avoid their use in tracklet building. The structure of the algorithm allows to make this selection on clusters once the tracklets have been reconstructed. After the tracklet reconstruction, a loop over the tracklets is performed. For each of the two clusters in the tracklet the check on the distance previously described is carried out: if the distance is within a fiducial elliptical window, those clusters are flagged. These flags will then be checked for the clusters in the following reconstructed tracklets: if at least one of the two clusters has been previously flagged, the tracklet is eliminated from the list of the reconstructed tracklets and is not stored. The distance

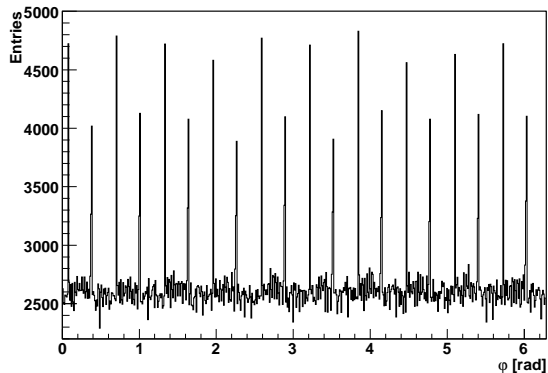


Figure 9: φ distributions for tracklets: the spikes are due to corresponding overlaps between adjacent modules both in the inner layer and in the outer layer in φ .

between clusters on adjacent modules is calculated in the $\Delta\varphi$ - Δz plane. The z coordinate of the clusters is calculated at the mean radius between the maximum and the minimum radii in the x - y plane for two modules in the overlap region. In order to fix the width of the windows in Δz and $\Delta\varphi$, the distributions in $\Delta\varphi$ and in Δz of clusters produced by the same primary that crosses two adjacent modules in each layer have been produced (Fig. 10). These have been compared to the same distributions for all pairs of clusters

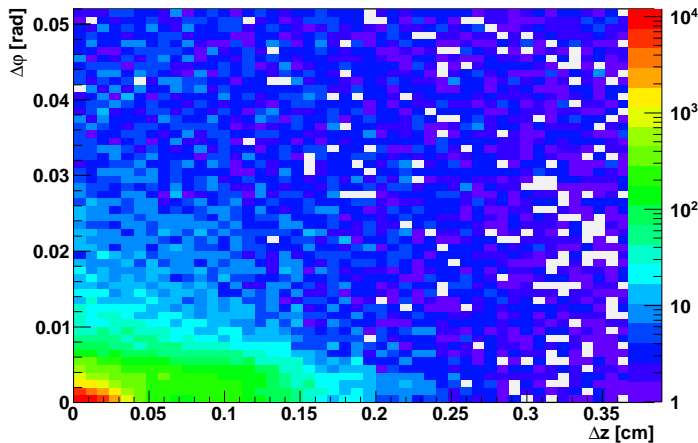


Figure 10: Distance in the $\Delta\varphi$ - Δz plane between two clusters produced by the same primary particles in two adjacent modules in the same SPD layer (inner layer).

on adjacent modules: the region around zero has the same entries of the previous plot. Therefore, cutting on the distance between clusters in adjacent modules is effective to select clusters produced by the same particle.

Two sets of cuts to flag the clusters in the SPD overlaps have been used to reconstruct

tracklets varying the cuts for the reconstruction itself as well.

In Tab. 8 the efficiencies and the tracklet composition are quoted for p-p events. In

$\Delta\varphi_{cut}$ (rad)	$\Delta\theta_{cut}$ (rad)	$\Delta\varphi_{SPDoverlaps}$ (rad)	$\Delta z_{SPDoverlaps}$ (cm)	Efficiency (%)	PP (%)	SS (%)	Combinatorics (%)
0.08	0.050	0.005	0.05	98.6	93.7	5.1	1.2
0.08	0.050	0.010	0.15	98.6	93.7	5.1	1.2
0.08	0.025	0.005	0.05	98.2	94.8	4.3	0.9
0.08	0.025	0.010	0.15	98.2	94.8	4.3	0.9
0.04	0.005	0.005	0.05	85.0	97.2	2.4	0.4
0.04	0.005	0.010	0.15	85.0	97.2	2.4	0.4

Table 8: *Efficiency of the optimized tracklet algorithm and tracklet composition for the p-p event sample cutting the clusters in the overlap regions of the SPD. Two different windows have been used to flag clusters, each of them for two different sets of the cuts for the tracklet reconstruction.*

p-p events the result does not change widening the cuts to eliminate tracklets in the SPD overlaps and both the efficiency and the tracklet composition remain constant compared to the efficiency of the algorithm without this option (Tab. 5). In Tab. 9 and Tab. 10 the efficiencies and the tracklet composition are quoted for Pb-Pb events. Comparing the

$\Delta\varphi_{cut}$ (rad)	$\Delta\theta_{cut}$ (rad)	$\Delta\varphi_{SPDoverlaps}$ (rad)	$\Delta z_{SPDoverlaps}$ (cm)	Efficiency (%)	PP (%)	SS (%)	Combinatorics (%)
0.08	0.050	0.005	0.05	80.4	68.8	2.8	28.4
0.08	0.050	0.015	0.15	79.6	68.4	2.7	28.9
0.08	0.025	0.005	0.05	82.7	73.3	2.8	23.9
0.08	0.025	0.015	0.20	82.2	73.1	2.7	24.2
0.04	0.005	0.005	0.05	73.8	82.8	2.1	15.1
0.04	0.005	0.015	0.20	73.4	82.6	2.1	15.3

Table 9: *Efficiency of the optimized tracklet algorithm and tracklet composition for the minimum bias Pb-Pb event sample cutting the clusters in the overlap regions of the SPD.*

reconstruction efficiency between the two sets of cuts, it can be concluded that the loss of efficiency is less than 1%. In the Pb-Pb case, the efficiency is also less than 1% lower than the efficiencies quoted in Tab. 6 and Tab. 7.

A reasonable choice for the cut widths is $\Delta\varphi_{SPDoverlap} = 0.01$ rad and $\Delta z_{SPDoverlaps} = 0.5$ cm: in Fig. 11 the comparison of the φ distributions obtained keeping and eliminating tracklets in the SPD overlaps, respectively, is shown for central Pb-Pb events.

The flagging of clusters in the overlap regions of the SPD can be optionally switched on in the reconstruction.

$\Delta\varphi_{cut}$ (rad)	$\Delta\theta_{cut}$ (rad)	$\Delta\varphi_{SPDoverlaps}$ (rad)	$\Delta z_{SPDoverlaps}$ (cm)	Efficiency (%)	PP (%)	SS (%)	Combinatorics (%)
0.08	0.050	0.005	0.05	71.2	61.0	1.9	37.1
0.08	0.050	0.015	0.15	70.7	61.1	1.9	36.9
0.08	0.025	0.005	0.05	74.2	65.2	2.0	32.8
0.08	0.025	0.015	0.20	73.6	65.3	2.0	32.6
0.04	0.005	0.005	0.05	67.5	74.7	1.8	23.5
0.04	0.005	0.015	0.20	67.0	74.7	1.8	23.5

Table 10: *Efficiency of the optimized tracklet algorithm and tracklet composition for the central Pb-Pb event sample cutting the clusters in the overlap regions of the SPD.*

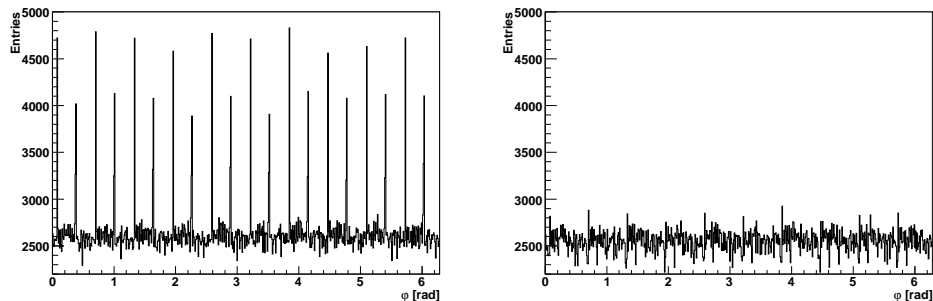


Figure 11: *Comparison between the φ distribution for tracklets (left panel) and the same distribution obtained implementing the search for clusters in overlapping modules, compatible with clusters produced by the same track (right panel).*

6 Conclusions

A method to reconstruct tracklets using particle hits in the two pixel layers of the inner tracking system has been developed. The performance, in terms of efficiency in finding tracklets associated to primary particles and contamination from combinatorial background, have been studied as a function of the angular selection cuts used to define the tracklets themselves. The main results are illustrated in this note.

References

- [1] ALICE ITS Technical Design Report, CERN/LHCC 99-12 (1999).
- [2] K. Aamodt *et al.*, JINST **3** (2008) S08002.
- [3] ALICE Physics Performance Report, Volume II, J. Phys. G: Nucl. Part. Phys. **32**, (2006), 1295-2040.
- [4] A. Dainese and M. Masera, ALICE Internal Note, ALICE-INT-2003-027.

- [5] M. Masera *et al.*, ALICE Internal Note, ALICE-INT-2009-018.
- [6] T. Virgili *et al.*, ALICE Internal Note, ALICE-INT-2002-043.
- [7] M. Nicassio *et al.*, ALICE Internal Note, ALICE-INT-2009-029.
- [8] J. F. Grosse-Oetringhaus, CERN-THESIS-2009-033.
- [9] PHOBOS Collaboration, B. B. Back *et al.*, “*Charged particle multiplicity near mid-rapidity in central Au + Au collisions at $s^{*}(1/2) = 56\text{-A/GeV}$ and 130-A/GeV ”*, *Phys. Rev. Lett.* **85** (2000) 3100.